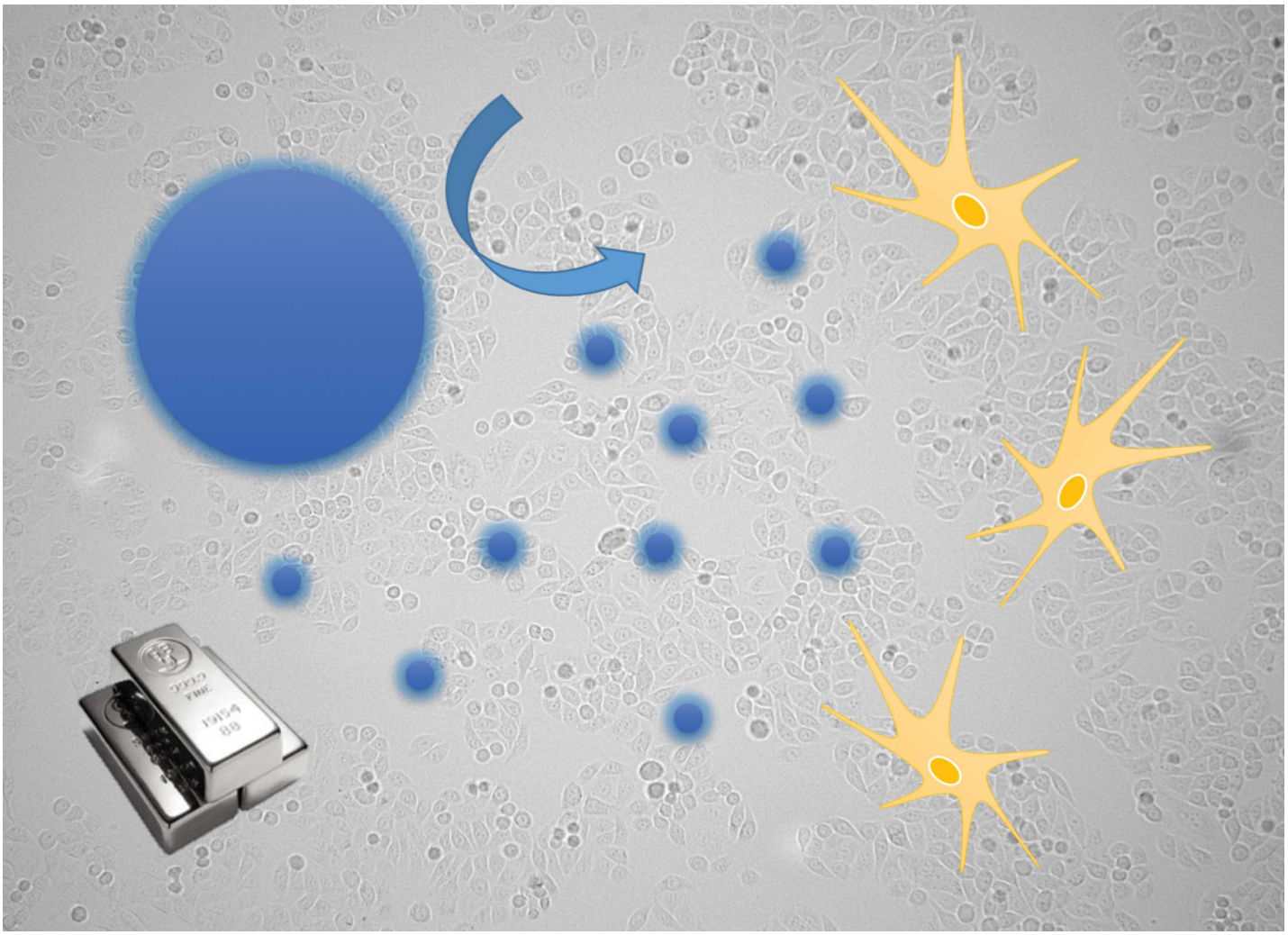

The groups of Prof. Epple from Inorganic Chemistry at Duisburg-Essen University (Germany), of Prof. Koeller from Surgical Research at Bochum University (Germany) and Prof. Vallet-Regi from Universidad Complutense Madrid (Spain) have a strong focus on the biological and medical properties of nanomaterials.

Title: The dissolution and biological effects of silver nanoparticles in biological media

Silver nanoparticles release toxic silver ions if oxidizing species are present, but their surface may be passivated by biomolecules.

As featured in:

See K. Loza *et al.*,
J. Mater. Chem. B, 2014, **2**, 1634.

ROYAL SOCIETY OF CHEMISTRY

www.rsc.org/MaterialsB

Registered charity number: 207890

Journal of Materials Chemistry B

PAPER

View Article Online
View Journal | View Issue

Cite this: *J. Mater. Chem. B*, 2014, **2**, 1634

The dissolution and biological effects of silver nanoparticles in biological media

K. Loza,[a] J. Diendorf,[a] C. Sengstock,[b] L. Ruiz-Gonzalez,[c] J. M. Gonzalez-Calbet,[c] M. Vallet-Regi,[c] M. Köller[b] and M. Epple*[a]

Silver ions and silver nanoparticles have a well-known biological effect that typically occurs in biological or environmental media of complex composition. Silver nanoparticles release silver ions if oxidizing species like molecular oxygen or hydrogen peroxide are present. The presence of glucose as a model for reducing sugars has only a small effect on the dissolution rate. In the presence of chloride ions, precipitation of silver chloride nanoparticles occurs. At physiological salt concentrations, no precipitation of silver phosphate occurs as the precipitation of silver chloride always occurs first. If the surface of a silver nanoparticle is passivated by cysteine, the dissolution is quantitatively inhibited. Upon immersion of silver nanoparticles in pure water for 8 months, leading to about 50% dissolution, no change in the surface was observed by transmission electron microscopy. A model for the dissolution was derived from immersion and dissolution experiments in different media and from high-resolution transmission electron microscopy. A literature survey on the available data on the dissolution of silver nanoparticles showed that only qualitative trends can be identified as the nature of the nanoparticles and of the immersion medium are practically never comparable. The dissolution effects were confirmed by cell culture experiments (human mesenchymal stem cells and neutrophil granulocytes) where silver nanoparticles that were stored under argon had a clearly lower cytotoxicity than those stored under air. They also led to a less formation of reactive oxygen species (ROS). This underscores that silver ions are the toxic species.

Received 6th November 2013
Accepted 10th January 2014

DOI: 10.1039/c3tb21569e

www.rsc.org/MaterialsB

Introduction

Silver nanoparticles are widely used in consumer products and in medicine due to their antibacterial action.[1–10] However, there is increasing evidence that the release of silver ions from nanoparticles is responsible for this biological effect. Xiu *et al.* showed in a very elegant experiment that silver nanoparticles did not show a bactericidal effect if the bacteria were cultivated under anaerobic conditions, *i.e.* when no dissolution of the nanoparticles occurred.[11] Studies on the dissolution behaviour were reported in a number of publications,[9,11–22] but there is no agreement on the dissolution behaviour in more complex media which are present, *e.g.* in biological systems and in the environment.

Based on our previous results on the dissolution of dispersed silver nanoparticles in pure water,[15] we have extended our studies to more complex media which are closer to the biological conditions in cell culture media and body fluids. We have analysed the dissolution kinetics and the nature of the silver nanoparticles after immersion in different media for up to 4000 h. Table 1 summarizes the results of dissolution experiments from the literature and from this study.

It must be stressed that it is not possible to monitor the dissolution of nanoparticles and their cytotoxicity in the same experiment. The nanoparticles will dissolve with a given kinetics, and the cells will react with some delay to the increasing silver concentration. Therefore, we have separated these two aspects by measuring the dissolution kinetics of the silver nanoparticles in more complex media and by studying the cytotoxicity of silver nanoparticles that were stored under argon (*i.e.* without released silver ions up to the start of the experiment). Summarizing these observations, we propose a model for the behaviour of silver nanoparticles and for the state of released silver ions under these conditions.

Experimental section

Synthesis of silver nanoparticles

PVP-coated silver nanoparticles were synthesized by reduction with glucose in the presence of PVP according to Wang *et al.*[24] Briefly, 2 g glucose and 1 g PVP were dissolved in 40 g water and heated to 90 °C. Then 0.5 g $AgNO_3$ dissolved in 1 mL water was

[a]*Inorganic Chemistry and Centre for Nanointegration Duisburg-Essen (CeNIDE), University of Duisburg-Essen, Universitaetsstr. 5-7, 45117 Essen, Germany. E-mail: matthias.epple@uni-due.de*

[b]*Bergmannsheil University Hospital/Surgical Research, Ruhr-University of Bochum, Buerkle-de-la-Camp-Platz 1, 44789 Bochum, Germany*

[c]*Departmento de Quimica Inorganica, Universidad Complutense, 28040 Madrid, Spain*

Table 1 Results of dissolution experiments of silver nanoparticles. Room temperature means 25 °C. Citrate-stabilized nanoparticles can be assumed to have a negative zeta potential, but this was not always stated in the references. The immersion medium was water in all cases with the stated additives. All experiments were carried out at neutral pH, unless specified otherwise

Functionalization of silver nanoparticles	Diameter/nm	Zeta potential/mV	Silver concentration/g L^{-1}	Temperature/°C	Immersion medium	Immersion time/h	Degree of dissolution/%	Ref.
Citrate	85	−30	0.32	25	Water	336	15	15
Citrate	85	−30	0.14	25	Water	410	12	15
Citrate	85	−30	0.32	37	Water	307	56	15
Citrate	85	−30	0.14	37	Water	444	53	15
Citrate	4.8	−45	0.002	25	Air-saturated distilled water, $[O_2] = 9.1$ mg L^{-1}; pH = 5.68	3000	~100	12
Citrate	4.8	−45	0.0002	25	Air-saturated distilled water, $[O_2] = 9.1$ mg L^{-1}; pH = 5.68	240	~100	12
Citrate	4.8	−45	0.00005	25	Air-saturated distilled water, $[O_2] = 9.1$ mg L^{-1}; pH = 5.68	120	~100	12
Citrate	4.8	−45	0.00005	4	Air-saturated distilled water, $[O_2] = 9.1$ mg L^{-1}; pH = 5.68	120	36	12
Citrate	4.8	−45	0.00005	37	Air-saturated distilled water, $[O_2] = 9.1$ mg L^{-1}; pH = 5.68	120	96	12
PVP	50	−17	0.22	5	Water	411	9	15
PVP	50	−17	0.1	5	Water	149	8	15
PVP	50	−17	0.05	5	Water	149	12	15
PVP	50	−17	0.35	25	Water	134	48	15
PVP	50	−17	0.1	25	Water	81	52	15
PVP	50	−17	0.05	25	Water	42	43	15
PVP	50	−17	0.35	37	Water	27	52	15
PVP	50	−17	0.1	37	Water	27	89	15
PVP	50	−17	0.05	37	Water	11	68	15
PVP	70	−22	0.35	25	Oxygen-free water	1660	2	This work
Citrate	4.8	−45	0.00005	25	Natural seawater, pH = 7.90	192	38	12
Citrate	20	—	0.0003	25	Modified ¼ Hoagland medium, $[O_2] = 7.8$ mg L^{-1}; pH = 5.6	336	40	21
Citrate	20	—	0.0006	25	Modified ¼ Hoagland medium, $[O_2] = 7.8$ mg L^{-1}; pH = 5.6	336	29	21
Citrate	40	—	0.0003	25	Modified ¼ Hoagland medium, $[O_2] = 7.8$ mg L^{-1}; pH = 5.6	336	21	21
Citrate	40	—	0.0006	25	Modified ¼ Hoagland medium, $[O_2] = 7.8$ mg L^{-1}; pH = 5.6	336	20	21
Citrate	80	—	0.0003	25	Modified ¼ Hoagland medium, $[O_2] = 7.8$ mg L^{-1}; pH = 5.6	336	10	21
Citrate	80	—	0.0006	25	Modified ¼ Hoagland medium, $[O_2] = 7.8$ mg L^{-1}; pH = 5.6	336	8	21
PVP	70	−22	0.35	25	0.9% NaCl	3670	8	This work
PVP	70	−22	0.35	25	PBS	3670	4	This work
PVP	39	Negative	1	25	0.01 M $NaNO_3$, pH = 7	720	1.9	18
PVP, sulphidated	39	Negative	1	25	0.01 M $NaNO_3$, pH = 7	730	*ca.* 0 to 0.27	18
PVP	70	−22	0.35	25	10 mM H_2O_2	1821	90	This work
Citrate	4.8	−45	0.002	25	Acetate buffer, pH 5.6	24	15	13
Citrate	4.8	−45	0.002	25	Acetate buffer, 0.4 mM citrate; pH 5.6	24	9	13

Table 1 (*Contd.*)

Functionalization of silver nanoparticles	Diameter/nm	Zeta potential/mV	Silver concentration/g L^{-1}	Temperature/°C	Immersion medium	Immersion time/h	Degree of dissolution/%	Ref.
Citrate	4.8	−45	0.002	25	Acetate buffer, 10 mM citrate; pH 5.6	24	7	13
Citrate	4.8	−45	0.002	25	Acetate buffer, 0.4 mM Na_2S; pH 5.6	24	<1	13
Citrate	4.8	−45	0.002	25	Acetate buffer, 4 mM 11-mercaptoundecanoic acid; pH 5.6	24	*ca.* 0	13
PVP	70	−22	0.35	25	1 g L^{-1} cysteine	4366	*ca.* 0	This work
PVP	70	−22	0.35	25	1 g L^{-1} glucose	4366	61	This work
Citrate	4.8	−45	0.00005	25	Boric acid and bicarbonate low ionic strength seawater buffer, pH = 7.90	192	54	12
Citrate	23	—	0.005	25	DMEM	22	*ca.* 75	20
Citrate	23	—	0.1	25	DMEM	22	*ca.* 7	20
PVP	23	—	0.005	25	DMEM	22	*ca.* 76	20
5 kDa PEG	23	—	0.005	25	DMEM	22	*ca.* 83	20
20 kDa PEG	23	—	0.005	25	DMEM	22	*ca.* 75	20
Dextran	23	—	0.005	25	DMEM	22	*ca.* 67	20
5 kDa PEG	23	—	0.1	25	DMEM	22	*ca.* 11	20
20 kDa PEG	23	—	0.1	25	DMEM	22	*ca.* 9	20
PVP	4–5	Negative	0.005	37	Synthetic gastric acid, pH = 1.12	24	~98	23
PVP	4–5	Negative	0.005	37	Pseudoextracellular fluid, pH = 7.52	24	~80	23

quickly added. The dispersion was kept at 90 °C for 1 h and then let to cool to room temperature. The particles were collected by ultracentrifugation (29 400*g*; 30 min), redispersed in pure water and collected again by ultracentrifugation. Thereby NO_3^-, excess glucose and its oxidation products, excess PVP, and excess Ag^+ were all removed. The silver nanoparticles were then redispersed in water by ultrasonication. The final silver concentration in all dispersions was determined by atomic absorption spectroscopy (AAS).

Poly(vinylpyrrolidone) (PVP K30, Povidon 30; Fluka, molecular weight 40 000 g mol^{-1}), silver nitrate (Roth, p.a.), sodium chloride (VWR, p.a.), D-(+)-glucose (Fluka, p.a.), cysteine (Merck, p.a.), and hydrogen peroxide (Sigma, p.a.) were used. Phosphate-buffered saline solution (PBS) was obtained from Gibco. RPMI 1640 was obtained from Gibco. LB medium was obtained from Sigma-Aldrich. Fetal calf serum (FCS) was obtained from Gibco. Ultrapure water was prepared with an ELGA Purelab ultra instrument.

Analytical methods

Scanning electron microscopy (SEM) was performed with a FEI Quanta 400 ESEM instrument in a high vacuum after sputtering with Au:Pd, if necessary. Energy-dispersive X-ray spectrometry was carried out with a Genesis 4000 instrument. Transmission electron microscopy (TEM) was carried out both with JEOL 400EX and JEOL 3000FEG electron microscopes, equipped with an Oxford LINK EDS analyser. The samples were ultrasonically dispersed in ethanol and then transferred to holey carbon-coated copper grids.

The hydrodynamic diameter and the zeta potential of the nanoparticles were measured by dynamic light scattering (DLS) using a Malvern Zetasizer Nano ZS. The polydispersity index (PDI) was below 0.3 in all cases. The concentration of silver was determined by atomic absorption spectroscopy (AAS; Thermo Electron Corporation, M-Series). The detection limit was 1 μg L^{-1}.

X-ray powder diffraction was carried out on a Bruker D8 Advance instrument in Bragg-Brentano mode with Cu Kα radiation (1.54 Å). Dissolved oxygen was measured with a WTW Oxi3250 instrument equipped with a CellOx 325 sensor.

Dialysis experiments were carried out in dialysis bags (Spectra/Por Biotech; cellulose ester; MWCO 100 000) filled with 4 mL silver nanoparticle dispersion (0.35 g L^{-1} Ag) and immersed in 396 mL ultrapure water. The dialysis was carried out under slow stirring with a magnetic stirrer at room temperature.

The dispersions of silver nanoparticles in different media were stirred at room temperature for 7 days. The nanoparticles and all precipitates were isolated by ultracentrifugation (24 900*g*; 30 min), redispersed in pure water and again subjected to ultracentrifugation. This procedure was repeated three times.

Simulation of the equilibrium of aqueous silver in the biological media was performed using Visual MINTEQ 3.0 (J.P. Gustafsson, Stockholm, 2011). The simulation was performed for 0.1 g L^{-1} dissolved silver. The model medium contained only inorganic salts. Solids were allowed to precipitate.

Preparation of stock and working solutions

PVP-coated spherical silver nanoparticles were dispersed in sterile ultrapure water at 1 g L^{-1} (1000 ppm) as stock solution. A solution of silver acetate with 1 g L^{-1} was the second stock solution. Both stock solutions were diluted with ultrapure water to prepare working stock solutions for the individual experiments at different silver concentrations (10–1000 ppm). The final concentrations were achieved by the addition of 50 μL of either silver nanoparticle or silver acetate working stock solutions to a 1 mL cell suspension prior to cultivation. Thereby the concentrations of other medium ingredients were kept constant in all experiments.

The final concentrations used for bacterial and cell culture tests were 50 μg mL^{-1}, 30 μg mL^{-1}, 25 μg mL^{-1}, 20 μg mL^{-1}, and 12.5 μg mL^{-1} for silver nanoparticles. The nanoparticles were freshly prepared and stored for 1 month at 7 °C before the biological tests. Ag-NPs were stored either under air or under argon to avoid oxidation and subsequent release of silver ions.[12,13,15,16,25]

All concentration values given in tables and figures refer to the mass of silver in the solution, regardless of its state (ions or nanoparticles).

Cell culture experiments

Human mesenchymal stem cells (hMSCs, 3rd to 7th passage, Lonza, Walkersville Inc., MD, USA) were cultured in cell culture medium RPMI/10% FCS using 24-well cell culture plates (Falcon, Becton Dickinson GmbH, Heidelberg, Germany). Cells were maintained at 37 °C in a humidified atmosphere with 5% CO_2. hMSCs were sub-cultivated every 7–14 days depending on the cell proliferation. Adherent cells were washed with phosphate-buffered saline solution (PBS, GIBCO, Life Technologies) and detached from the culture flasks by the addition of 0.2 mL cm^{-2} 0.25% trypsin/0.1% ethylenediaminetetraacetic acid (EDTA, Sigma-Aldrich, Taufkirchen, Germany) for 5 min at 37 °C. Subsequently, the hMSCs were collected and washed twice with RPMI/10% FCS. Subconfluently growing hMSCs were incubated at 37 °C in the presence or absence of different concentrations of silver nanoparticles for 24 h under cell culture conditions.

The viability and the morphology of the incubated hMSCs were analysed using calcein-acetoxymethylester (calcein-AM, Calbiochem, Schwalbach, Germany) fluorescence staining. After incubation for 24 h, the nanoparticle-treated cells and silver ion-treated cells were washed twice with RPMI and incubated with calcein-AM (1 μM) at 37 °C for 30 min under cell culture conditions. Subsequently, the adherent cells were washed again with RPMI and analysed by fluorescence microscopy (Olympus MVX10, Olympus, Hamburg, Germany). Fluorescence microphotographs were taken (Cell P, Olympus) and digitally processed using Adobe Photoshop® 7.0. The cell morphology was analysed by phase-contrast microscopy (Olympus MVX). In this method, living cells give rise to green fluorescence.

Polymorphonuclear neutrophil granulocytes (PMNs), which are known to be potent producers of ROS, were isolated by using a single-step procedure that was based on a discontinuous double-Ficoll gradient described by English and Andersen.[26] Cell counting was performed using Tuerk staining solution (Sigma-Aldrich). The isolated cells were adjusted to 1×10^6 cells mL^{-1} in RPMI cell culture medium supplemented with L-glutamine (0.3 g L^{-1}), sodium bicarbonate (2.0 g L^{-1}), 10% (v/v) FCS, and 20 mM *N*-(2-hydroxyethyl)-piperazine-*N*′-(2-ethanesulfonic acid) (HEPES, Sigma-Aldrich).

To monitor the generation of ROS from silver-treated PMNs, the oxidant-sensitive dye, DCFH-DA (2′,7′-dichlorofluorescein-diacetate), was used, as described by Hsin *et al.*[27] and Carlson *et al.*[28] After 1 h exposure to Ag-NPs or silver ions or 10 μM fMLP (formyl-methionyl-leucyl-phenylalanine), 10 min before DCFH-DA addition, prior to analysis, as a positive control, the cells were centrifuged at 370*g* for 5 min at room temperature. The supernatants were discarded, and the pellets were carefully resuspended. Subsequently, the cells were incubated with 20 μM DCFH-DA (resuspended in RPMI/10% FCS) for 30 min in the dark (37 °C, 5% CO_2). After incubation, the cells were washed, centrifuged and fixed with 1.5% paraformaldehyde. The fluorescent signal was monitored by flow cytometry.

Bacterial culture experiments

Bacterial tests were performed with *Staphylococcus aureus* (DSMZ 1104) obtained from the DSMZ (German Collection of Microorganisms and Cell Cultures). *S. aureus* was grown in BHI broth (brain-heart infusion broth, bioMérieux, Nürtingen, Germany) overnight at 37 °C in a water bath. Bacterial concentrations of overnight cultures were measured using a Densichek® (bioMérieux, Lyon, France) turbidity photometer. The calculation of bacterial counts was based on turbidity standard solutions (McFarland scale).

The antimicrobial activity of nanoparticulate silver was tested using standard methods which determine the minimum inhibitory concentration (MIC) and the minimum bactericidal concentration (MBC). The MIC was determined in RPMI 1640 (Life Technologies) containing 10% (v/v) fetal calf serum (FCS, Life Technologies) and L-glutamine (0.3 g L^{-1}, Life Technologies), and defined as the lowest silver concentration required to inhibit bacterial growth (no visible growth) in 2 mL plastic macrodilution test tubes. Therefore, working silver stock solutions (50 μL) were added to 1 mL of the respective liquid culture medium, and different cell numbers (10^3 to 10^6 mL^{-1}) of bacteria were used for inoculation. Cells were incubated in a cell culture incubator (RPMI/10% FCS) in the presence of 5% carbon dioxide in a humidified atmosphere at 37 °C overnight.

The minimum bactericidal concentration (MBC) was subsequently determined by plating 100 μL aliquots of the MIC samples on blood agar plates. The MBC was defined as the lowest silver concentration that completely prevented colony forming units (CFU) on the agar plate.

Statistical analysis

Data are expressed as mean ± standard deviation of at least three independent experiments. Analysis of the data distribution was performed using Student's *t*-test to analyse the

significance of differences between the treated group and the control group (without silver exposure). *P* values of less than 0.05 were considered statistically significant.

Results and discussion

Dissolution experiments of silver nanoparticles

The dissolution of silver nanoparticles was monitored by long-term experiments using dialysis bags containing nanoparticles which were permeable only for silver ions. Previous studies have shown that the dissolution is fast at the beginning and slows down over time, leading to incompletely dissolved particles.[15] Of course, an immersion in pure water is far from realistic conditions in biological or environmental media. As these media are very complex in nature and many components will act simultaneously on the silver nanoparticles, we have simplified the system by the addition of various model compounds. We have added various compounds that are also present in biological media to the immersion medium and measured the dissolution curves. In particular, we added chloride and phosphate as typical anions that can lead to the precipitation of sparingly soluble silver salts (AgCl and Ag_3PO_4), glucose as a reducing sugar, and cysteine as a model for sulphur-containing proteins. As dissolved oxygen is the only agent that can dissolve metallic silver under these conditions, we also varied the oxygen content of the solution. Finally, H_2O_2 was used as a strongly oxidizing compound.

Representative dissolution curves for PVP-coated silver nanoparticles are shown in Fig. 1.

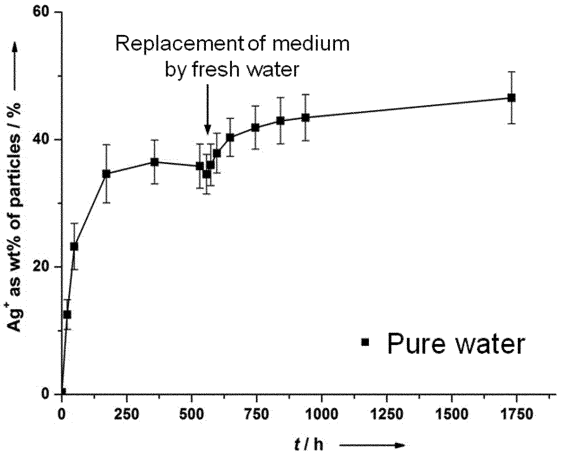

Fig. 2 Partial dissolution of silver nanoparticles (PVP-coated; 70 nm), immersed in pure water, with exchange of the surrounding medium by fresh water. The access of oxygen was allowed at all times.

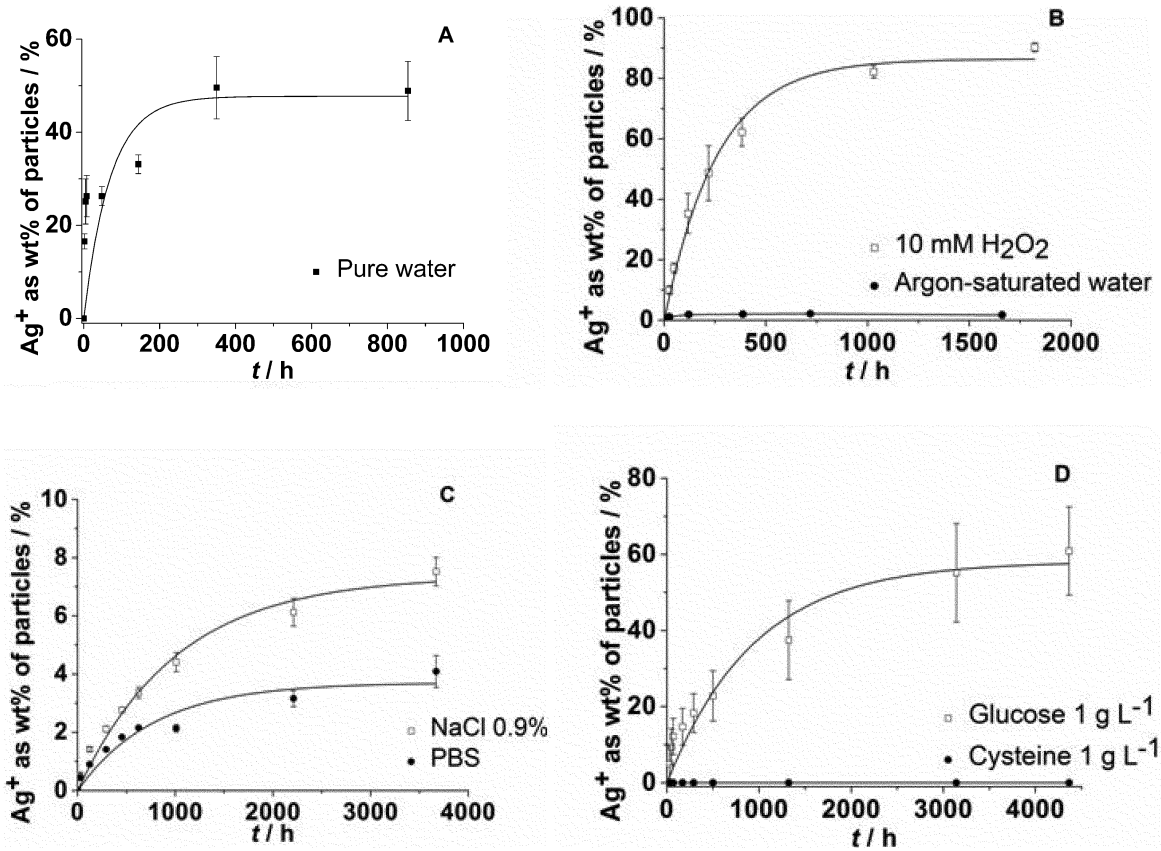

Fig. 1 Dissolution of silver nanoparticles immersed in pure water (A: data taken from ref. 15), degassed, argon-saturated water under an argon atmosphere, and in water with 10 mM H_2O_2 (B), in aqueous NaCl (0.9%) or in PBS (C), and in the presence of either cysteine (aq.: 1 g L^{-1}) or glucose (aq.: 1 g L^{-1}) (D).

Table 2 Results of the immersion experiments after 7 days. PVP-stabilized silver nanoparticles (AgNPs) with a hydrodynamic diameter of 70 nm were used at a concentration of 0.1 g L^{-1}. All solid products were isolated by ultracentrifugation. The particles were analysed by SEM, EDX and XRD. The maximum possible amount of dissolved Ag^+ was calculated using the chemical equilibrium software Visual MinteQ 3.0

Medium	Particles found in the ultracentrifugate, with diameter	Maximum possible concentrations of Ag^+ in the immersion medium/μg L^{-1}	Concentration of Cl^-/M
Glucose (2 g L^{-1})	Ag (70 nm)		0
NaCl (0.9%)	Ag (70 nm), AgCl (400–800 nm)	0.225	0.154
NaCl (0.9%) + glucose (2 g L^{-1})	Ag (70 nm), AgCl (200–500 nm)	0.225	0.154
PBS	Ag (70 nm), AgCl (200–300 nm)	0.250	0.139
PBS + glucose (2 g L^{-1})	Ag (70 nm), AgCl (200–500 nm)	0.250	0.139
RPMI 1640 medium/10% FCS	Ag (70 nm), AgCl (110–140 nm)	0.327	0.108
LB medium	Ag (70 nm), AgCl (250–300 nm)	0.372	0.085

The dissolution requires the presence of dissolved oxygen as it is obvious from Fig. 1B. If no oxygen is present, only a very small fraction of silver is dissolved, possibly by traces of oxygen in the experimental setup. An oxidizing agent like H_2O_2 clearly enhances the dissolution. The presence of dissolved NaCl, either in pure form or as PBS, strongly slows down the dissolution (Fig. 1C), probably due to the formation of silver chloride on the particle surface (passivation). Cysteine has a clearly inhibiting effect with almost no dissolution of the silver nanoparticles. Glucose has a decelerating effect but leads to a similar final dissolved fraction (Fig. 1D). This suggests that cysteine adsorbs onto the silver nanoparticle surface with its thiol group and prevents the subsequent oxidation of silver. In contrast, glucose slows down the dissolution, but clearly does not prevent the oxidation on a longer time scale.

Incomplete dissolution of nanoparticles

The fact that silver nanoparticles dissolve only partially in the presence of air unless a very strong oxidizing agent like H_2O_2 is present is astonishing, but corresponds to previous results by us[15] and Zhang *et al.*[21] We will discuss this observation in the following paragraph.

There appears to be agreement in the literature that dissolved oxygen is the oxidizing species for silver under normal circumstances. A complexation by organic ligands may facilitate the oxidation of silver by shifting the equilibrium, but cannot explain the dissolution by itself. Another remarkable observation is the only partial dissolution of silver nanoparticles, even after a long time.[15] This may be due to a lack of the oxidizing species, *i.e.* oxygen. We have therefore measured the oxygen concentration in the air-saturated surrounding water and found to be 5.2 mg O_2 per L, *i.e.* 160 μM O_2. This is more than enough to oxidize 1.4 mg of metallic silver in the system (13 μmol dissolved in 400 mL, *i.e.* 32 μM). We have also performed the dissolution in pure water for 500 h and then exchanged the surrounding medium by fresh water. The dissolution starts again, but not as much as expected and leads to a new "equilibrium" (Fig. 2).

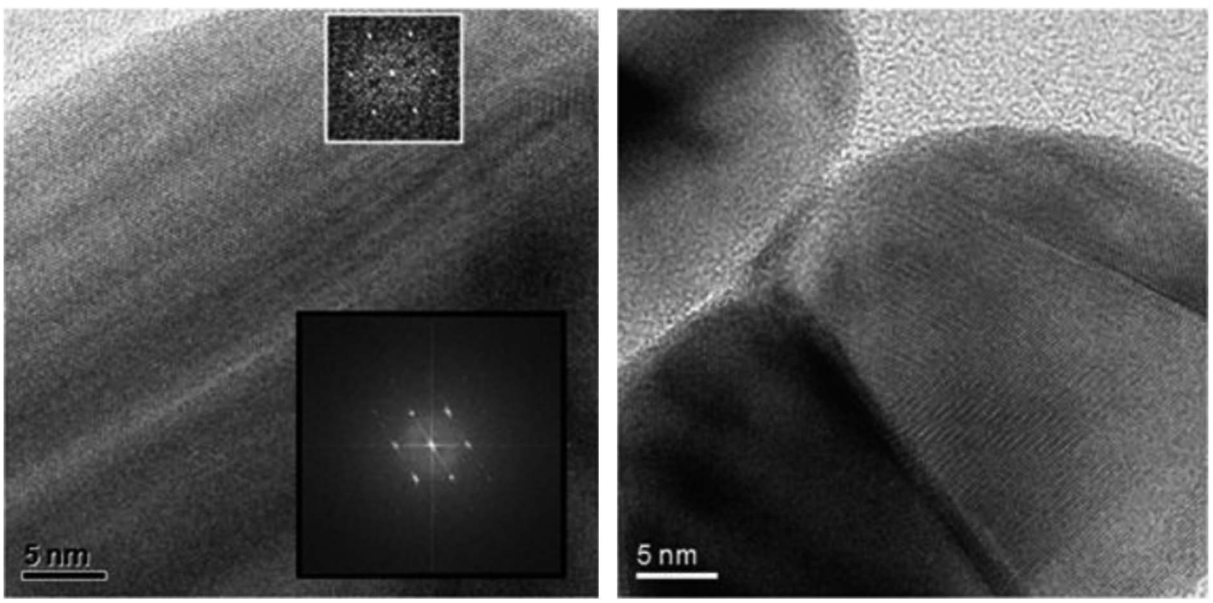

Fig. 3 High-resolution transmission electron micrographs of freshly prepared silver nanoparticles (PVP-coated; 70 nm) (left) and of silver nanoparticles after 8 months immersion in water (right). No change in the surface is recognizable. The electron diffraction image insets in the left indicate the presence of metallic silver.

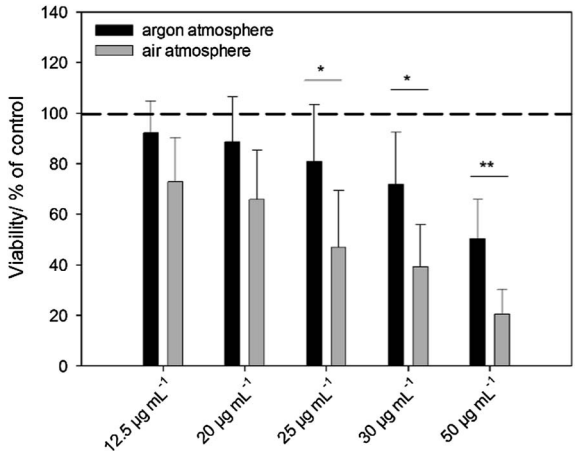

Fig. 4 Influence of silver nanoparticles (PVP-stabilized, 70 nm) stored either under argon or air on the viability of human mesenchymal stem cells (hMSCs). The cells were treated with different concentrations of silver nanoparticles for 24 h under cell culture conditions. The silver amount of added particles is given in μg mL^{-1}. Vital cells (green fluorescence) were quantified by digital image processing (phase analysis). The data are expressed as mean ± standard deviation ($N = 5$) given as the percentage of the control (cells cultured without nanoparticles).

This demonstrates that it is not the presence of oxygen alone which leads to a dissolution of silver. An explanation might be a kind of surface passivation during immersion. High-resolution transmission electron microscopy on immersed silver nanoparticles was therefore performed to investigate the presence of any passivating surface layer after immersion in water. Fig. 3 shows representative images. A change of the nanoparticle surface was never detectable, ruling out the presence of a surface passivation.

Behaviour of silver nanoparticles in complex media

In order to better understand the processes during immersion, we have extended these studies by mixing silver nanoparticle dispersions with media of increasingly biological nature and studying the (nano-)particulate reaction products. The solutions/dispersions were stirred for equilibration and then subjected to ultracentrifugation. All precipitates and nanoparticles were isolated by this way and then analysed by scanning electron microscopy, energy-dispersive X-ray spectroscopy and X-ray powder diffraction. This gives an integral view on all the particulate species that are present after long-term immersion. The results are summarized in Table 2. The original silver nanoparticles were found practically unchanged after the immersion, indicating that it had only partially dissolved.

The results show that the released silver ions are mainly precipitated as AgCl if chloride is present. We have also computed the maximum concentration of silver in the presence of various inorganic ions and found that less than one μg of silver per litre can be present in thermodynamic equilibrium. This, of course, neglects the influence of organic species that may act as coordinating ligands and also a possible non-equilibrium state of the dispersion. The initially present silver nanoparticles were recovered in all cases. Silver phosphate was never observed, probably due to the moderate pH (around 7) at which phosphate is mostly protonated to hydrogen phosphate and dihydrogen phosphate.

Cell and bacterial culture experiments with silver nanoparticles stored under air and under argon

Our hypothesis that the release of silver ions determines silver toxicity was confirmed by cell culture experiments. If the

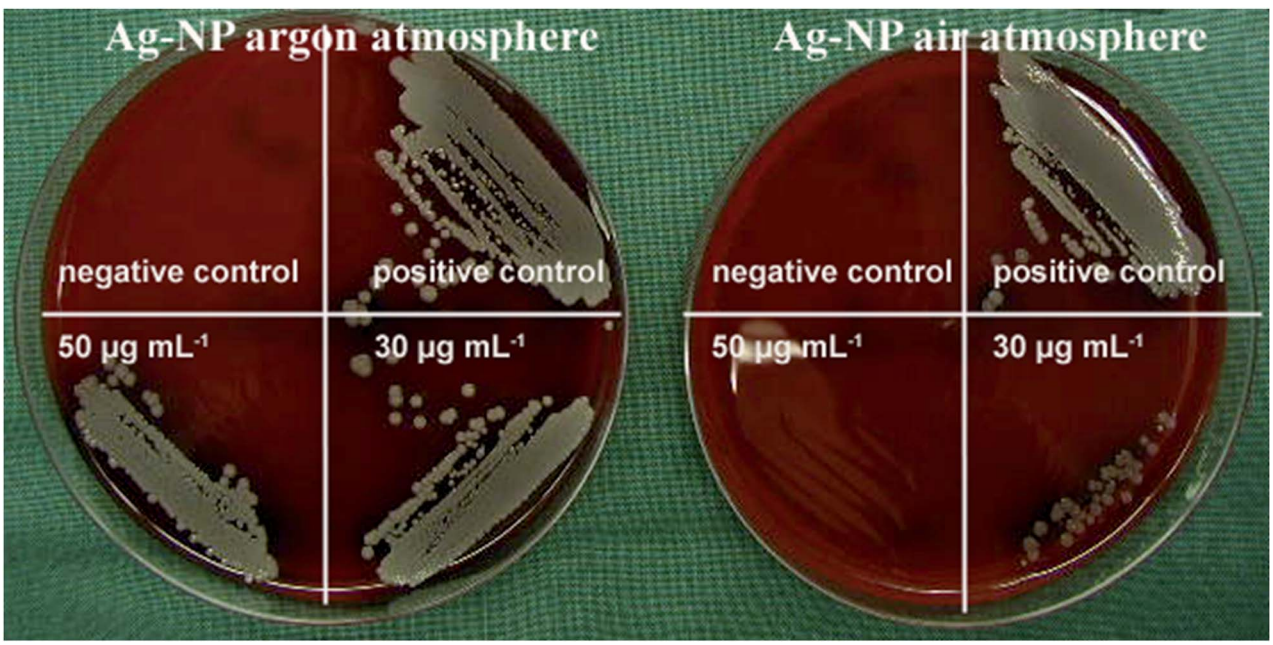

Fig. 5 Representative images of *S. aureus* colonies on blood agar plates. *S. aureus* (10^6 cells mL^{-1} in medium) was treated without (*S. aureus* in pure medium: positive control; pure medium: negative control) or with 50 μg mL^{-1} or 30 μg mL^{-1} of silver nanoparticles stored either under argon or air for 24 h under cell culture conditions. Subsequently, the bacteria were plated and incubated for further 24 h at 37 °C.

Table 3 Summary of toxic silver concentrations (MBC; Ag-NPs synthesized under argon or air) given in μg mL^{-1} of silver. The toxicity of silver decreased when higher numbers of bacteria were used for inoculation and when particles were synthesized under an argon atmosphere

Number of bacteria used for inoculation	Ag nanoparticles stored under an argon atmosphere	Ag nanoparticles stored under air
1×10^6	>50	>50
1×10^5	>50	50
1×10^4	>50	30–25
1×10^3	25	25–20

nanoparticles were stored under argon, they did not partially dissolve and therefore were much less toxic towards tissue-like cells than the same particles stored under air (Fig. 4). In addition, the same results were obtained by microbiological experiments using *S. aureus* where oxidized silver nanoparticles were much more toxic than those stored under air (Fig. 5 and Table 3). Of course, the particles will dissolve after coming into contact with air, therefore they will become increasingly bactericidal (and cytotoxic) with time.

Formation of reactive oxygen species (ROS)

We and others have shown that reactive oxygen species (ROS) were generated from cells as a consequence of silver nanoparticle exposure and that the formation of ROS contributes to silver induced cell toxicity.[29–32] Air-stored silver nanoparticles induced a pronounced increase in cellular ROS formation compared to the same amount of argon-stored silver nanoparticles (Fig. 6A and B). The addition of silver acetate (the same silver concentration as the nanoparticles) induced the highest release in ROS under these conditions comparable to the standard cell stimulus formyl-methionyl-leucyl-phenylalanine (fMLP).

Silver nanoparticles enter the cell by endocytosis and end up first in an endosome and then in a lysosome.[33] There, they encounter acidic conditions with a pH between 4 and 5.[34] Liu and Hurt have studied the dissolution of silver nanoparticles at different pH and found an increase of the ion release at lower pH. We can therefore assume that the silver nanoparticles will undergo accelerated dissolution after endosomal uptake. However, the time in the cell culture medium is much longer than the time in the lysosome, therefore the toxic action of silver is probably due to both effects.

A model for the behaviour of silver nanoparticles in complex media

The typically applied methods for silver determination are AAS or ICP-MS, and the separation of silver nanoparticles and silver ions is typically accomplished by dialysis or nanofiltration. In general, although there are a number of studies where the dissolution kinetics of dispersed silver nanoparticles was measured, they are practically incomparable (Table 1). The properties of the nanoparticles were rather diverse (*e.g.* size, charge, functionalization), and it is very likely that this strongly influences their dissolution behaviour. Furthermore, the immersion media are different and not easily comparable between the individual data points. Finally, it can be safely assumed that the total silver concentration will influence the dissolution process, as critical factors like the solubility product of silver chloride or the reduction potential of silver ions directly depend on the concentration. However, some conclusions can be drawn, mainly by comparing results within one set of experiments, *i.e.* from one reference.

Liu *et al.* described the dissolution of silver nanoparticles in acetate buffer in the presence of citrate anions, sodium sulphide and 11-mercaptoundecanoic (MUA) acid and found that sulphidation and MUA reduced the dissolution rate to undetectable values.[13] They also investigated the role of humic and fulvic acids, dissolved oxygen, natural and low salt sea

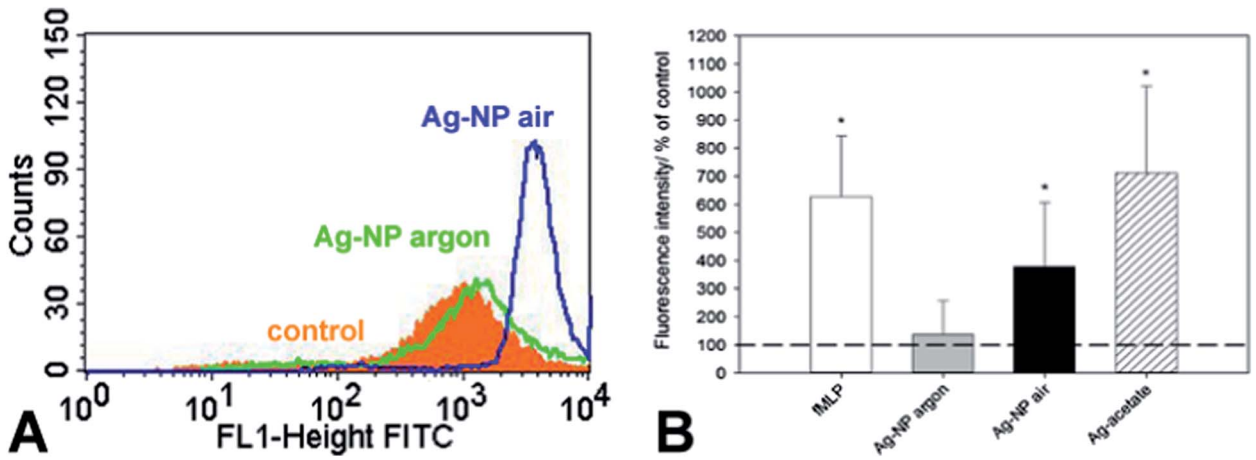

Fig. 6 Generation of ROS in neutrophil granulocytes after treatment with different silver species or formyl-methionyl-leucyl-phenylalanine (fMLP). Ag-NPs stored either under argon or air and silver ions, as analysed by flow cytometry. After 1 h of incubation, the fluorescence intensity of dichlorofluorescein (DCF) was assessed (A: representative flow cytometric histogram; control: cells cultured without silver). Quantitative data are expressed as the mean ± SD ($N = 3$ independent experiments, B), given as the percent of the control (cells cultured without silver, broken line). The asterisk (*) indicates significant differences compared to the control (*$p < 0.05$).

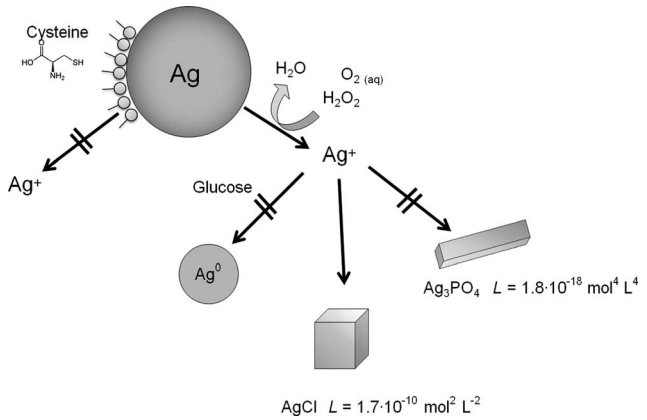

Fig. 7 Summary of all experiments and proposed dissolution/precipitation mechanisms.

water and showed that the addition of organic matter can suppress the release of silver ions.[12] Levard *et al.* investigated the role of a surface sulphidation process and found that at a high ratio of sulphur to silver, the released silver content decreased to hardly detectable values.[18] Zook *et al.* measured the dissolution in cell culture medium (DMEM) and found a fractional dissolution of different polymer coated silver nanoparticles. The dissolution was enhanced in biological media in comparison to inorganic salt solutions which is probably due to complexation of the released silver ions.[20] Zhang *et al.* considered size effects on the dissolution kinetics in quarter-strength Hoagland medium and concluded the dependence of size and concentration on the release rate. Smaller particles were found to dissolve faster.[21] The fate of silver nanoparticles in synthetic gastric fluid and wound fluid was studied by Liu *et al.* They reported a rapid dissolution in gastric acid in comparison to pseudoextracellular fluid and also found an interaction with thiol- and selenide-containing biomolecules. They proposed the formation of secondary thiol- and selenide-containing nanoparticles after partial dissolution in the gastrointestinal tract.[23]

Our own observations and the collected literature data led us to the model that is depicted in Fig. 7.

Conclusions

From the reported experiments and the available literature on the dissolution of silver nanoparticles, we conclude that

(1) Metallic silver is oxidized by dissolved molecular oxygen.

(2) Thiol- or selenide-containing compounds can block the particle surface and prevent the dissolution (in our studies represented by a cysteine molecule).

(3) Once silver ions are released into the solution, they are rapidly precipitated as silver chlorides, apparently not on the surface of the initial silver particles, but as separate particles. The equilibrium concentration of Ag^+ is very small (<1 ppb).

(4) Silver phosphate is not formed if chloride is present.

(5) Reducing sugars (here: glucose) slow down, but do not prevent the oxidative dissolution of silver.

(6) Organic molecules can lead to a complexation of silver ions and thereby accelerate the dissolution.

(7) Silver nanoparticles do not dissolve completely in the presence of molecular oxygen. A stronger oxidation agent like H_2O_2 is necessary for a complete dissolution.

(8) The toxic species for eukaryotic cells and for bacteria are silver ions that are released after oxidation of silver nanoparticles. These lead to the formation of reactive oxygen species (ROS).

Acknowledgements

We thank the Deutsche Forschungsgemeinschaft (DFG) for financial support of this project within the Priority Program NanoBio Responses (SPP1313). We thank the network of excellence agening.net (CS2010-11384-E) for generous support.

Notes and references

1 Y. Teow, P. V. Asharani, M. P. Hande and S. Valiyaveettil, *Chem. Commun.*, 2011, **47**, 7025–7038.
2 B. Nowack, H. F. Krug and M. Height, *Environ. Sci. Technol.*, 2011, **45**, 1177–1183.
3 F. Gottschalk and B. Nowack, *J. Environ. Monit.*, 2011, **13**, 1145–1155.
4 S. Galdiero, A. Falanga, M. Vitiello, M. Cantisani, V. Marra and M. Galdiero, *Molecules*, 2011, **16**, 8894–8918.
5 B. Simoncic and B. Tomsic, *Text. Res. J.*, 2010, **80**, 1721–1737.
6 K. Chaloupka, Y. Malam and A. M. Seifalian, *Trends Biotechnol.*, 2010, **28**, 580–588.
7 J. W. Alexander, *Surg. Infect.: Sel. Antibiot. Ther.*, 2009, **10**, 289–292.
8 X. Chen and H. J. Schluesener, *Toxicol. Lett.*, 2008, **176**, 1–12.
9 G. A. Sotiriou and S. E. Pratsinis, *Curr. Opin. Chem. Eng.*, 2011, **1**, 3–10.
10 S. Chernousova and M. Epple, *Angew. Chem., Int. Ed.*, 2013, **52**, 1636–1653.
11 Z. M. Xiu, Q. B. Zhang, H. L. Puppala, V. L. Colvin and P. J. J. Alvarez, *Nano Lett.*, 2012, **12**, 4271–4275.
12 L. Liu and R. H. Hurt, *Environ. Sci. Technol.*, 2010, **44**, 2169–2175.
13 J. Liu, D. A. Sonshine, S. Shervani and R. H. Hurt, *ACS Nano*, 2010, **4**, 6903–6913.
14 X. Li, J. J. Lenhart and H. W. Walker, *Langmuir*, 2010, **26**, 16690–16698.
15 S. Kittler, C. Greulich, J. Diendorf, M. Köller and M. Epple, *Chem. Mater.*, 2010, **22**, 4548–4554.
16 C. M. Ho, S. K. W. Yau, C. N. Lok, M. H. So and C. M. Che, *Chem. – Asian J.*, 2010, **5**, 285–293.
17 G. A. Sotiriou and S. E. Pratsinis, *Environ. Sci. Technol.*, 2010, **44**, 5649–5654.
18 C. Levard, B. C. Reinsch, F. M. Michel, C. Oumahi, G. V. Lowry and G. E. Brown, *Environ. Sci. Technol.*, 2011, **45**, 5260–5266.
19 C. M. Ho, C. K. Wong, S. K. W. Yau, C. N. Lok and C. M. Che, *Chem. – Asian J.*, 2011, **6**, 2506–2511.

20 J. M. Zook, S. E. Long, D. Cleveland, C. L. A. Geronimo and R. I. MacCuspie, *Anal. Bioanal. Chem.*, 2011, **401**, 1993–2002.
21 W. Zhang, Y. Yao, N. Sullivan and Y. Chen, *Environ. Sci. Technol.*, 2011, **45**, 4422–4428.
22 Z. M. Xiu, J. Ma and P. J. J. Alvarez, *Environ. Sci. Technol.*, 2011, **45**, 9003–9008.
23 J. Y. Liu, Z. Y. Wang, F. D. Liu, A. B. Kane and R. H. Hurt, *ACS Nano*, 2012, **6**, 9887–9899.
24 H. Wang, X. Qiao, J. Chen and S. Ding, *Colloids Surf., A*, 2005, **256**, 111–115.
25 C. N. Lok, C. M. Ho, R. Chen, Q. Y. He, W. Y. Yu, H. Sun, P. K. H. Tam, J. F. Chiu and C. M. Che, *J. Biol. Inorg. Chem.*, 2007, **12**, 527–534.
26 D. English and B. R. Andersen, *J. Immunol. Methods*, 1974, **5**, 249–252.
27 Y. H. Hsin, C. F. Chen, S. Huang, T. S. Shih, P. S. Lai and P. J. Chueh, *Toxicol. Lett.*, 2008, **179**, 130–139.
28 C. Carlson, S. M. Hussain, A. M. Schrand, L. K. Braydich-Stolle, K. L. Hess, R. L. Jones and J. J. Schlager, *J. Phys. Chem. B*, 2008, **112**, 13608–13619.
29 O. Choi and Z. Q. Hu, *Environ. Sci. Technol.*, 2008, **42**, 4583–4588.
30 H. J. Park, J. Y. Kim, J. Kim, J. H. Lee, J. S. Hahn, M. B. Gu and J. Yoon, *Water Res.*, 2009, **43**, 1027–1032.
31 C. Greulich, J. Diendorf, J. Geßmann, T. Simon, T. Habijan, G. Eggeler, T. A. Schildhauer, M. Epple and M. Köller, *Acta Biomater.*, 2011, **7**, 3505–3514.
32 D. Guo, L. Zhu, Z. Huang, H. Zhou, Y. Ge, W. Ma, J. Wu, X. Zhang, X. Zhou, Y. Zhang, Y. Zhao and N. Gu, *Biomaterials*, 2013, **34**, 7884–7894.
33 C. Greulich, J. Diendorf, T. Simon, G. Eggeler, M. Epple and M. Köller, *Acta Biomater.*, 2011, **7**, 347–354.
34 P. R. Gil, M. Nazarenus, S. Ashraf and W. J. Parak, *Small*, 2012, **8**, 943–948.